Self-association studies of the bifunctional N-acetylglucosamine-1-phosphate uridyltransferase from Escherichia coli

ARTICLE *in* PROTEIN SCIENCE · APRIL 2011

Impact Factor: 2.85 · DOI: 10.1002/pro.608 · Source: PubMed

4 AUTHORS, INCLUDING:

Jean-François Trempe
McGill University
42 PUBLICATIONS **1,203** CITATIONS

Self-association studies of the bifunctional *N*-acetylglucosamine-1-phosphate uridyltransferase from *Escherichia coli*

Jean-François Trempe,* Solomon Shenker, Guennadi Kozlov, and Kalle Gehring

Department of Biochemistry, Groupe de recherche axé sur la structure des protéines, McGill University, Montreal, QC, Canada H3G 0B1

Received 29 November 2010; Revised 31 January 2011; Accepted 1 February 2011
DOI: 10.1002/pro.608
Published online 2 March 2011 proteinscience.org

Abstract: The *N*-acetylglucosamine-1-phosphate uridyltransferase (GlmU) is a key bifunctional enzyme in the biosynthesis of UDP-GlcNAc, a precursor in the synthesis of cell wall peptidoglycan. Crystal structures of the enzyme from different bacterial strains showed that the polypeptide forms a trimer through a unique parallel left-handed beta helix domain. Here, we show that the GlmU enzyme from *Escherichia coli* forms a hexamer in solution. Sedimentation equilibrium analytical ultracentrifugation demonstrated that the enzyme is in a trimer/hexamer equilibrium. Small-angle X-ray scattering studies were performed to determine the structure of the hexameric assembly and showed that two trimers assemble through their N-terminal domains. The interaction is mediated by a loop that undergoes a large conformational change in the uridyl transferase reaction, a feature that may affect the enzymatic activity of GlmU.

Keywords: GlmU; SAXS; AUC; self-association; beta helix

Introduction

The protein encoded by the *glmU* gene in *Escherichia coli* is a bifunctional enzyme that catalyzes the two last steps in the *de novo* biosynthesis of UDP-GlcNAc, a precursor used in bacterial cell wall synthesis.[1,2] The enzyme first uses acetyl-CoA to transfer an acetyl group to glucosamine-1-phosphate to yield *N*-acetyl-glucosamine-1-phosphate (GlcNAc-1-P). UTP is then used to add an uridyl group on the product of the first reaction to form UDP-GlcNAc and pyrophosphate. The two enzymatic activities are contained within two distinct domains of the GlmU protein and are independent of each other.[3,4] The acetyl transferase activity is carried out by the C-terminal domain, which adopts a trimeric left-handed parallel beta helix (LβH) fold.[5,6] The uridyl transferase activity is contained within the globular N-terminal domain, which is part of the nucleotide triphosphate transferase superfamily of enzymes that resemble the Rossman fold and require magnesium for catalysis.[1,5,7]

Crystal structures of GlmU reported in the presence of different substrates and from various bacterial organisms have enabled the elucidation of its enzymatic mechanism.[5,6,8–12] All share the same characteristic trimeric structure where the acetyl transferase active site is located at the interface between two adjacent LβH monomers. The uridyl transferase active site, located in the nucleotide-binding pocket of the N-terminal domain, is located far from the acetyl transferase site, in accordance with biochemical studies that showed no substrate channeling was occurring in the enzyme.[1,3] In the crystal structures of GlmU from *E. coli*,[5,6] *Streptococcus pneumoniae*,[8,9] and *Haemophilus influenzae*,[11] the

Grant sponsor: Canadian Institutes of Health Research Genomics; Grant number: GSP-48370; Grant sponsor: CIHR postdoctoral fellowship (J.F.T.); Grant sponsor: Chercheur National of the Fonds de la recherché en santé du Québec K.G.

**Correspondence to:* Jean-François Trempe, Department of Biochemistry, Groupe de recherche axé sur la structure des protéines, McGill University, Montreal, QC, Canada H3G 0B1. E-mail: jean.trempe@mail.mcgill.ca

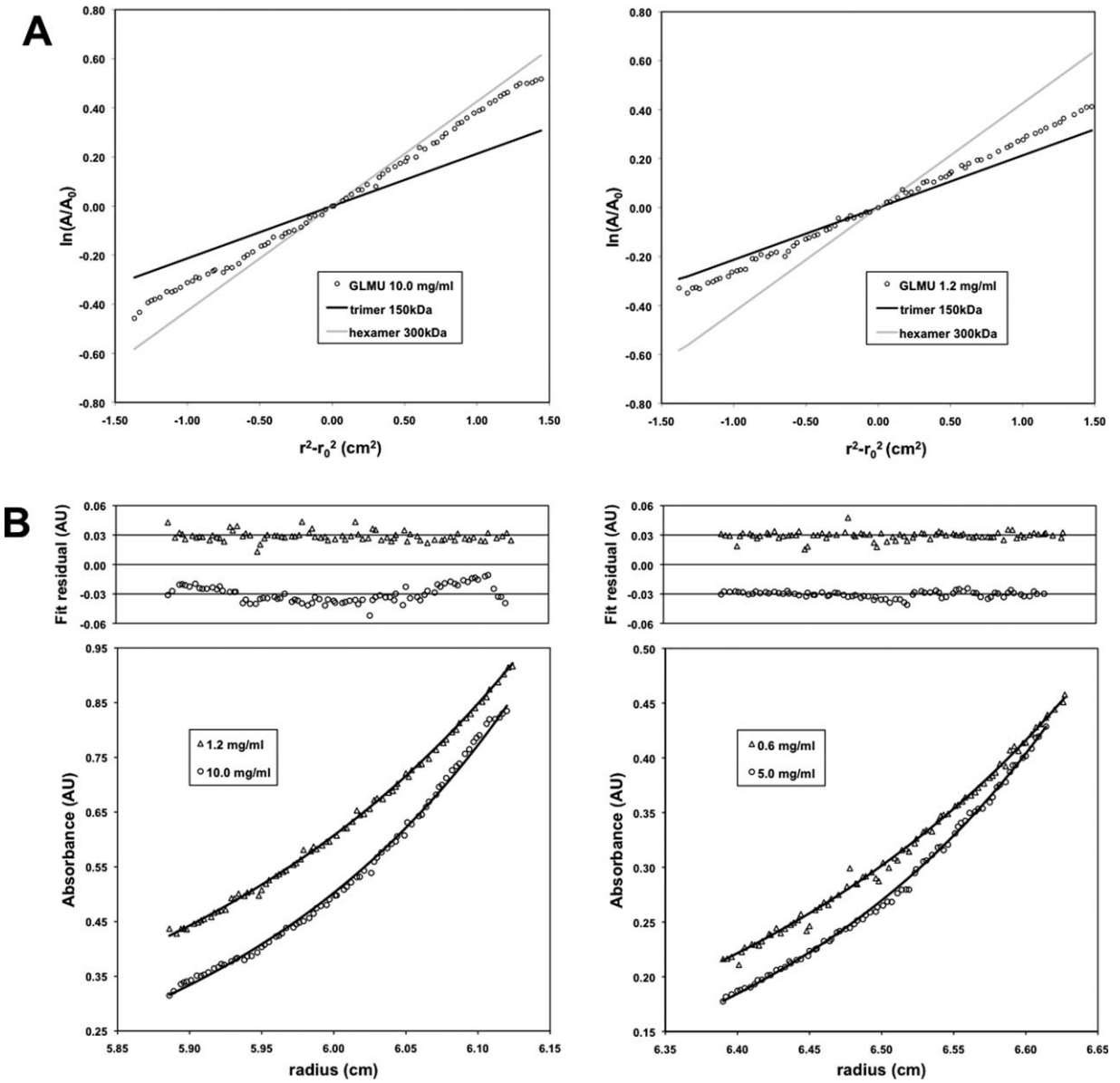

Figure 1. Sedimentation equilibrium analytical ultracentrifugation of GlmU. (A) Plots of $r^2 - r_0^2$ versus $ln(A/A_0)$ from sedimentation equilibrium AUC data of GlmU. Data acquired at 10 mg mL^{-1} (left) and 1.2 mg mL^{-1} (right) reveal a concentration-dependent oligomerization of GlmU. Predicted curves for GlmU trimer and hexamer assemblies are shown as black and grey lines, respectively. (B) Sedimentation equilibrium AUC data at four different GlmU concentrations were fitted to a simple self-association model of GlmU trimers and hexamers. An equilibrium dissociation constant of 24 ± 11 μM was obtained using a global fit. Fit residuals are shown on top and offset by ±0.03 AU for display purposes.

N-terminal domain was shown to adopt an open conformation in the apo or uridyl/UMP/UDP-bound form, and a closed conformation when bound to UDP-GlcNAc, supporting a model where a conformational change drives the uridyl transfer reaction.

Here, we characterize the oligomeric state of the *E. coli* GlmU in solution using small-angle X-ray scattering and analytical ultracentrifugation. We find that GlmU forms a specific hexameric structure through a reversible concentration-dependent self-association of GlmU trimers *via* the N-terminal domain. This hexameric form is consistent with crystal contacts observed in the crystal structure of full-length *E. coli* GlmU.[6,10] We discuss the potential implications of the GlmU oligomerization on its enzymatic activity.

Results and Discussion

The oligomerization state of the *E. coli* GlmU in solution was first investigated using sedimentation equilibrium analytical ultracentrifugation (AUC). The characteristic log(*C*) *versus* r^2 plot at low concentration (<1.2 mg mL^{-1}) showed a linear relationship with a slope and predicted molecular weight slightly greater than expected for a trimer [Fig. 1(A), right]. Moreover, higher concentrations showed

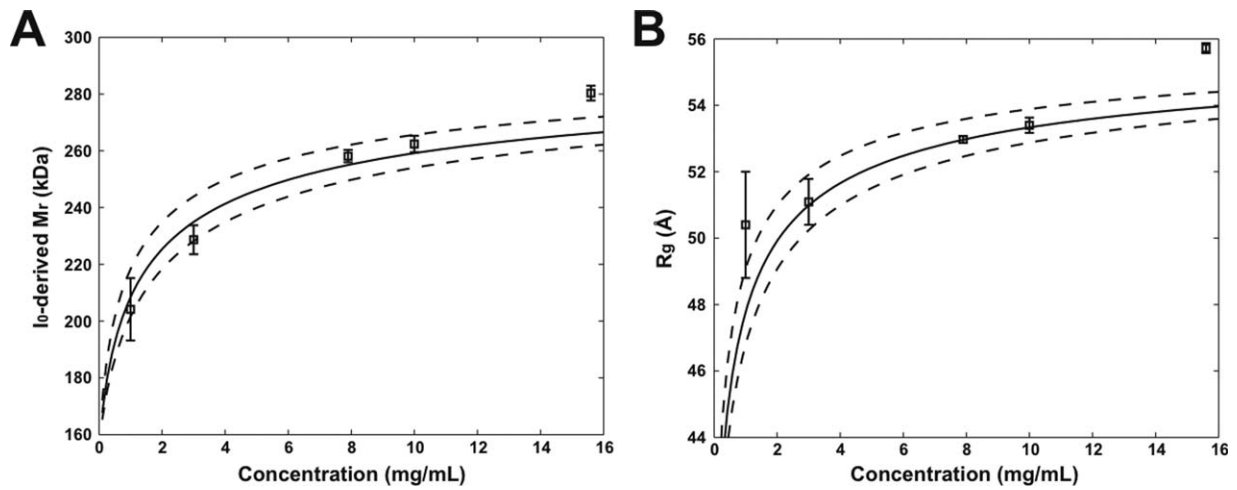

Figure 2. Guinier plot-derived SAXS parameters of GlmU at different concentrations. (A) Molecular weights derived from I_0 (A) and radius of gyration (B) values calculated from Guinier plots of SAXS profiles acquired on GlmU at different concentrations (squares). Experimental uncertainties are shown as capped vertical bars. Theoretical SAXS profiles of trimer (150 kDa) and hexamer (300 kDa) mixtures were generated to estimate the apparent Guinier plot-derived molecular weight at different concentrations using a K_d of 15 μM (plain line), ±5 μM (dashed lines). Theoretical profiles were generated using the hexamer 1 (head-to-head; see Fig. 3) from the *E. coli* GlmU crystal structure (PDB code 1HV9)[6], since the two hexameric forms observed in the structure have different R_g values (56 Å vs. 63 Å for hexamer 1 and 2, respectively).

increasingly greater slopes and a small deviation from linearity, indicating a concentration-dependent oligomerization [Fig. 1(A), left]. Indeed, the data at four different concentrations could be globally fitted to a model where two GlmU trimers self-associate to form a hexamer [Fig. 1(B)] with an equilibrium dissociation constant (K_d) of 24 ± 11 μM.

SAXS data were collected on GlmU at different concentrations and showed a concentration-dependent radius of gyration (R_g) and I_0 (Fig. 2). Notably, the R_g values are significantly higher than the value of 38 Å calculated for the trimer in the crystal structure of *E. coli* GlmU (PDB 1HV9). The molecular weight values derived from I_0 are higher than the trimeric molecular weight (150 kDa) and, like the R_g values, increase with concentration. Assuming a simple trimer/hexamer self-association model, the apparent Guinier-plot derived I_0 and R_g parameters can be generated from mixtures of trimeric and hexameric assemblies of GlmU. The estimated trimer/hexamer ratios were used to derive a K_d of 15 ± 5 μM, in agreement with the value derived from AUC. The data set collected at 16 mg mL^{-1} showed sign of aggregation when pair-distance distribution function were calculated and was excluded from the analysis. At 10 mg mL^{-1}, the I_0-derived molecular weight is close to that of the hexamer (300 kDa) and, thus, is used to probe its structure.

Possible models for the quaternary structure of a hexameric GlmU were derived by applying crystallographic symmetry operations to the trimeric structure of full-length *E. coli* GlmU.[6] Two different hexameric assemblies with 32-point symmetry can be derived from the crystal structure, as described in the original article [Fig. 3(A), right]. The GlmU trimers can either associate via their N-terminal "head" domains (hexamer 1) or stack through their C-terminal LβH "tail" domains (hexamer 2). To determine which of these assemblies GlmU forms in solution, a pair-distance distribution function was computed from the 10 mg mL^{-1} SAXS data and compared with theoretical curves calculated for the different assemblies [Fig. 3(A)]. The resulting curves show that the hexameric head-to-head assembly is the most likely oligomeric form. This was confirmed by performing a SAXS-derived *ab initio* shape reconstruction using the program DAMMIN[13], which clearly shows a head-to-head oligomeric arrangement where the N-terminal domains contact each other and form an inner cage [Fig. 3(B)].

To confirm that the SAXS data can be modeled by a reversible self-association of GlmU trimer and head-to-head hexamer, the data acquired at different GlmU concentrations were fitted to mixtures of trimer and either of the two hexameric forms. SAXS curves were computed for different fractions and the Chi^2 fit to the experimental data was calculated for every fraction [Fig. 4(A)]. At 10 mg mL^{-1}, the best fit was obtained with mole fractions of 0.1 of trimer and 0.9 of the head-to-head hexamer [Fig. 4(A), left]. At 0.8 mg mL^{-1}, the best fit was obtained with a mole fraction 0.4 of trimer and 0.6 of the head-to-head hexamer [Fig. 4(A), right]. At all mole fractions, the fit with the tail-to-tail arrangement was poor with a Chi^2 above 4 [Fig. 4(A), left] and a poor fit in the critical low angle region [Fig. 4(C)]. Overall, the SAXS data demonstrate that GlmU assembles into a head-to-head hexamer in solution.

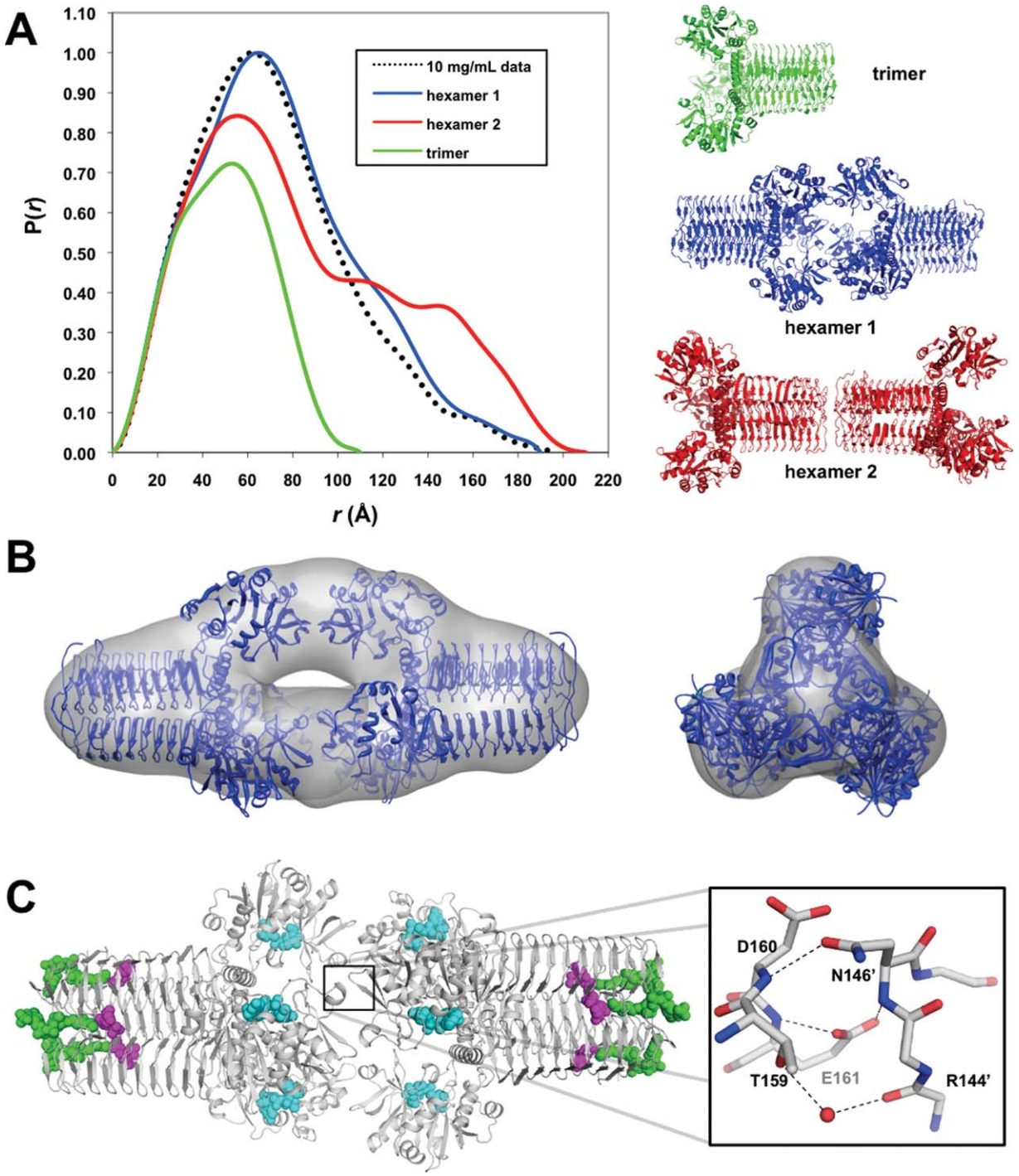

Figure 3. GlmU forms a hexamer through its N-terminal head domain. (A) The experimental pair-distance distribution function (PDDF) of a concentrated GlmU solution (10 mg mL^{-1}) is compared with the PDDF calculated for different assemblies observed in the crystal structure of GlmU (PDB code: 1HV9)[6]. The corresponding models are displayed on the right. (B) *Ab initio* SAXS reconstruction of GlmU using SAXS data acquired at 10 mg mL^{-1}. Twenty models were generated using DAMMIN and averaged using DAMAVER. A volumetric map was computed from the bead model using the SITUS package and displayed as a contoured surface using CHIMERA. The hexamer 1 (blue cartoon) form was superimposed on the volumetric map using CHIMERA. (C) Positions of substrates/products and interactions in the hexameric head-to-head assembly of GlmU. The hexameric assembly derived from the crystal structure of *E. coli* GlmU (white cartoon) in complex with desulfo-CoA (green), GlcNAc-1-P (magenta), and UDP-GlcNAc (cyan) is shown on top (PDB code: 2OI7)[10]. Details of the interactions between the N-terminal "head" domains are shown as sticks below, with dashed lines representing hydrogen bonds. The red sphere represents a water molecule. Residues labeled with (') belong to a different two-fold symmetry related domain.

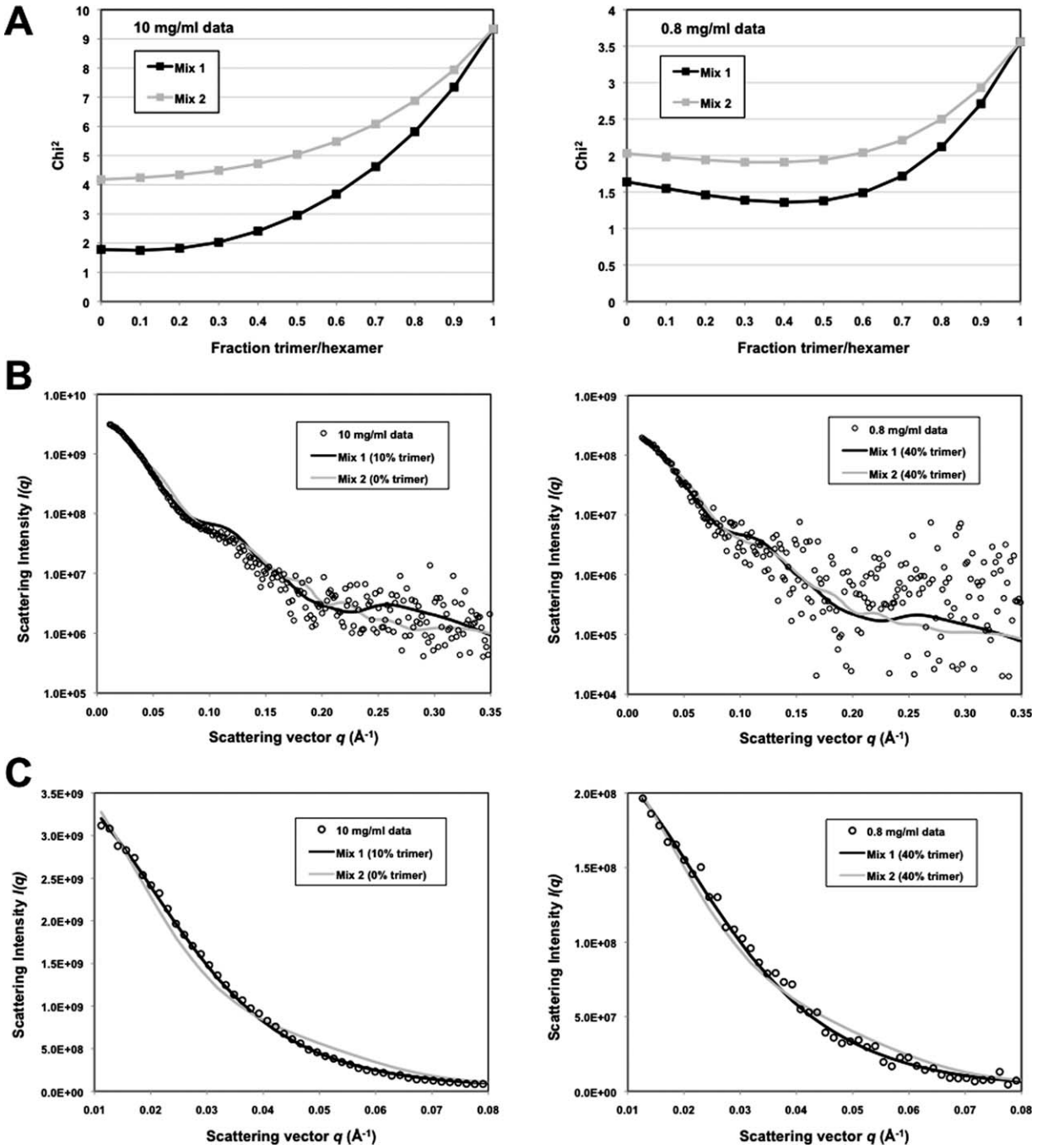

Figure 4. SAXS data fitting using mixtures of trimer and hexamer assemblies. (A) SAXS profiles were computed for different fractions of trimer/hexamer 1 (mix 1; black) or trimer/hexamer 2 (mix 2; grey) and fitted to the experimental SAXS data for GlmU at 10 mg mL^{-1} (left) and 0.8 mg mL^{-1} (right). The resulting Chi^2 values are plotted as a function of the molar fraction of trimer to total GlmU. (B) SAXS profiles q versus log(I) for fractions that best fit the data are shown along with the experimental SAXS data at 10 mg mL^{-1} (left) and 0.8 mg mL^{-1} (right). (C) Same as in (B) for the small angle region ($q < 0.08$) and using linear scale for $I(q)$.

In the crystal structure of *E. coli* GlmU (PDB 1HV9)[6], lattice contacts between the N-terminal domains consist of a network of hydrogen bonds between a small helix formed by residues 159–161 and a loop formed by residues 144–147, both located in the upper N-terminal lobe [Fig. 3(C)]. The total buried surface area at the interface between the two trimers is modest (800 $Å^2$) and has low hydrophobicity, with a positive solvation free energy of 1.5 kcal mol^{-1} upon complex formation as calculated using the PISA server.[14] Nonetheless, the same contacts were observed in all crystal structures of *E. coli* GlmU, including the truncated form of GlmU[5] and the full-length protein[6,10] that were crystallized in the absence or presence of different substrates and products. Moreover, the head-to-head hexameric

form was also observed in GlmU from *Mycobacterium tuberculosis* crystallized in the unbound and GlcNAc-1-P or UDP-GlcNAc-bound forms (PDB 3D98, 3D8V, 2QKX).[12] This raises the possibility that the hexameric form could be a conserved feature of GlmU. However, the residues at the hexamerization interface are not conserved between *E. coli* and *M. tuberculosis*, and the head-to-head arrangement was not observed in the crystal structures of GlmU from *H. influenzae*[11] and *S. pneumoniae*.[8,9] Nonetheless, the preponderance of hexameric assemblies in GlmU orthologues may reflect a quaternary structure that would normally be stabilized in a higher order metabolic complex through an, as yet, unidentified factor.

Similar head-to-head hexameric structures have been observed in solution for the related GDP-mannose pyrophosphorylase (GMP)[15] as well as in the crystal structure of the serine acetyltransferase (SAT)[16], which both have trimeric LβH domains. The SAT enzyme is part of the cysteine synthase multi-enzyme complex and forms a stable homohexamer (dimer of trimers) with a total buried surface area of 4450 Å^2 between its non-catalytic N-terminal domains. The function of the hexameric form of SAT (if any) remains unknown.[16] However, the occurrence of head-to-head hexamers in several enzymes that contain the trimeric LβH domain suggests that it may confer a specific function to those enzymes.

One possible implication of hexamerization in GlmU could be an altered enzymatic activity. The interactions between the N-terminal domains were earlier proposed to induce a bend in the hinge between the N-terminal and C-terminal domains that would prevent the conformational change required for divalent metal binding at the uridyl transferase active site.[6] Moreover, the loop residues that mediate hexamerization in both *E. coli*[6] and *M. tuberculosis*[12] GlmU enzymes undergo a large conformational change upon substrate binding that drives the uridyl transferase reaction.[5,6,8,9,11] Assuming that the one conformation is stabilized in the hexameric form, the uridyl transferase activity of GlmU could be allosterically inhibited at high concentrations of the enzyme. The self-association of GlmU trimer into hexamer is thus likely to be physiologically relevant. GlmU is an abundant protein in *E. coli*, with approximately 2500 molecules per cell.[2] Assuming that the molecules are uniformly distributed across the cytoplasmic volume (0.5 μm^3), the intracellular concentration of GlmU trimers is therefore ~3 μM. This number is only marginally below the equilibrium dissociation constant of ~15–20 μM and implies that a significant fraction of GlmU (~19–23%) would adopt the hexameric form *in vivo*. This fraction would be even higher in cellular locations with high local concentration of GlmU or if the hexamer form is stabilized in a higher order metabolic complex. Since the hexamer is formed through a loop involved in the uridyl transferase reaction, we hypothesize that changes in the ratio of GlmU trimer *versus* hexamer may regulate the rate of UDP-GlcNAc synthesis.

In conclusion, we have shown using AUC and SAXS that the bifunctional enzyme GlmU from *E. coli* self-associates in solution to form a specific hexameric structure in equilibrium with the previously characterized trimeric structure. The interactions between GlmU trimers are mediated by a loop in the N-terminal domain involved in the uridyl transferase reaction and therefore hexamer formation may affect the enzymatic activity of GlmU.

Materials and Methods

Sample preparation

The *E. coli* GlmU coding sequence (residues 2–456) was cloned in the pFO4 vector, a derivative of the pET15b vector (GE Healthcare), and transformed in BL21 (DE3) *E. coli* cells for protein expression with an N-terminal His_6-tag (MGSSHHHHHHGS). Cells were grown in LB medium to OD_{600}~0.8 at 37°C and protein expression was induced using 0.5 m*M* IPTG at 30°C for 3 h. Cells were resuspended in 50 m*M* Tris/HCl pH 8.0 and lysed by sonication. The protein was affinity-purified using Ni-NTA agarose (Qiagen) and eluted using 200 m*M* imidazole. The protein was further purified by size-exclusion chromatography using a 16/60 Superdex 200 column (GE Healthcare) in TBS buffer (10 m*M* Tris-HCl, 50 m*M* NaCl, 5 m*M* $MgCl_2$, 5 m*M* 2-mercaptoethanol, pH 7.5). The protein was concentrated using a 10 kDa Amicon filter unit (Millipore) and the concentration was determined by UV spectrophotometry (e_{280} = 32,890 M^{-1} cm^{-1}; M_r = 50,388 Da).

Sedimentation equilibrium analytical ultracentrifugation

AUC experiments were performed at 20°C using a Beckman Coulter XL-I analytical ultracentrifuge. The samples were spun with an angular velocity of 5000 rpm until concentration gradients reached equilibrium (~24 h). The protein concentration gradients were monitored by UV at 303 nm (5 and 10 mg mL^{-1}) and 290 nm (0.6 and 1.2 mg mL^{-1}). Samples at 0.6 and 1.2 mg mL^{-1} were collected directly from gel filtration and were not concentrated, whereas the 5 and 10 mg mL^{-1} were concentrated following gel filtration. Data were fitted to a self-association model according to the following equation:

$$C(r) = C_0 \exp\left[\frac{M(1-\nu_1\rho)\varpi^2}{2RT}(r^2 - r_0^2)\right] + \frac{2C_0^2}{K_d}\exp\left[\frac{2M(1-\nu_1\rho)\varpi^2}{2RT}(r^2 - r_0^2)\right]$$

where r is the radius, $C(r)$ is the concentration, C_0 is the concentration at r_0 (reference radius), M is the molecular weight (151,164 g mol^{-1}), ν_1 is the protein partial specific volume (0.735 cm^3 g^{-1}), r is the buffer density (1.005 g cm^{-3}), ϖ is the angular velocity, R is the gas constant (8.314472 $\times$ 10^7 erg·K^{-1} mol^{-1}), T is the absolute temperature (293.15 K), and K_d is the equilibrium dissociation constant. The partial specific volume ν_1 was estimated from the GlmU crystal structure and allowed to vary by $\pm$0.005 cm^3 g^{-1} to evaluate uncertainty in the dissociation constant.

Small-angle X-ray scattering

The SAXS measurements were carried out using an Anton Paar SAXSess camera equipped with a PANalytical PW3830 X-ray generator and a Roper/Princeton CCD detector. The beam length was set to 18 mm, and the beam profile was recorded using an image plate for subsequent desmearing. Data were collected at 20°C for different protein concentrations and exposure times: 10.0 mg mL^{-1} (1 h), 7.9 mg mL^{-1} (2 h), 3.0 mg mL^{-1} (2 h) and 0.8 mg mL^{-1} (8 h). The sample at 0.8 mg mL^{-1} was collected directly from the gel filtration peak and was not concentrated. Dark current correction, scaling, buffer subtraction, binning, and desmearing were performed using the Anton Paar software SAXSquant 3.0. R_g and I_0 values were estimated from Guinier plots in the range 0.012–0.025 Å^{-1}. A standard measurement was performed on a lysozyme solution (10.0 mg mL^{-1} in 40 m*M* sodium acetate, 50 m*M* NaCl, pH 3.8) collected for 1 h at 20°C. The I_0-derived molecular weights were calculated from the lysozyme standard (14.3 kDa) using the equation:

$$M_G = M_L \frac{I_{OG} C_L}{I_{OL} C_G}$$

where M_G and M_L are the GlmU and lysozyme molecular weights, I_{0G} and I_{0L} are the GlmU and lysozyme I_0 values, and C_G and C_L are the GlmU and lysozyme concentrations (mass/volume). Scattering profiles from atomic models were computed using CRYSOL[17] and pair-distance distribution functions were computed using GNOM[18]. The DAMMIN *ab initio* reconstruction was performed using the PDDF of GlmU at 10 mg mL^{-1} (D_{max} = 190 Å), assuming P32 point symmetry[13]. Twenty models with good agreement to the data were averaged using DAMAVER[19] and a volumetric map was computed from the beads model using the SITUS package[20]. The SAXS profiles of trimer/hexamer fractions and Chi^2 were computed using an in-house Microsoft Excel routine.

Acknowledgment

The authors thank the Biophysics platform at IRIC (Université de Montréal) and Nadeem Siddiqui for assistance with the AUC experiment.

References

1. Mengin-Lecreulx D, van Heijenoort J (1994) Copurification of glucosamine-1-phosphate acetyltransferase and *N*-acetylglucosamine-1-phosphate uridyltransferase activities of *Escherichia coli*: characterization of the glmU gene product as a bifunctional enzyme catalyzing two subsequent steps in the pathway for UDP-*N*-acetylglucosamine synthesis. J Bacteriol 176:5788–5795.
2. Mengin-Lecreulx D, van Heijenoort J (1993) Identification of the glmU gene encoding *N*-acetylglucosamine-1-phosphate uridyltransferase in *Escherichia coli*. J Bacteriol 175:6150–6157.
3. Gehring AM, Lees WJ, Mindiola DJ, Walsh CT, Brown ED (1996) Acetyltransfer precedes uridylyltransfer in the formation of UDP-N-acetylglucosamine in separable active sites of the bifunctional GlmU protein of *Escherichia coli*. Biochemistry 35:579–585.
4. Pompeo F, Bourne Y, van Heijenoort J, Fassy F, Mengin-Lecreulx D (2001) Dissection of the bifunctional *Escherichia coli* N-acetylglucosamine-1-phosphate uridyltransferase enzyme into autonomously functional domains and evidence that trimerization is absolutely required for glucosamine-1-phosphate acetyltransferase activity and cell growth. J Biol Chem 276: 3833–3839.
5. Brown K, Pompeo F, Dixon S, Mengin-Lecreulx D, Cambillau C, Bourne Y (1999) Crystal structure of the bifunctional N-acetylglucosamine 1-phosphate uridyltransferase from *Escherichia coli*: a paradigm for the related pyrophosphorylase superfamily. EMBO J 18: 4096–4107.
6. Olsen LR, Roderick SL (2001) Structure of the *Escherichia coli* GlmU pyrophosphorylase and acetyltransferase active sites. Biochemistry 40:1913–1921.
7. Sivaraman J, Sauve V, Matte A, Cygler M (2002) Crystal structure of *Escherichia coli* glucose-1-phosphate thymidylyltransferase (RffH) complexed with dTTP and Mg2+. J Biol Chem 277:44214–44219.
8. Sulzenbacher G, Gal L, Peneff C, Fassy F, Bourne Y (2001) Crystal structure of Streptococcus pneumoniae *N*-acetylglucosamine-1-phosphate uridyltransferase bound to acetyl-coenzyme A reveals a novel active site architecture. J Biol Chem 276:11844–11851.
9. Kostrewa D, D'Arcy A, Takacs B, Kamber M (2001) Crystal structures of Streptococcus pneumoniae *N*-acetylglucosamine-1-phosphate uridyltransferase, GlmU, in apo form at 2.33 A resolution and in complex with UDP-*N*-acetylglucosamine and Mg(2+) at 1.96 Å resolution. J Mol Biol 305:279–289.
10. Olsen LR, Vetting MW, Roderick SL (2007) Structure of the *E. coli* bifunctional GlmU acetyltransferase active site with substrates and products. Protein Sci 16:1230–1235.
11. Mochalkin I, Lightle S, Zhu Y, Ohren JF, Spessard C, Chirgadze NY, Banotai C, Melnick M, McDowell L. (2007) Characterization of substrate binding and catalysis in the potential antibacterial target N-acetylglucosamine-1-phosphate uridyltransferase (GlmU). Protein Sci 16:2657–2666.
12. Zhang Z, Bulloch EM, Bunker RD, Baker EN, Squire CJ (2009) Structure and function of GlmU from Mycobacterium tuberculosis. Acta Cryst D 65:275–283.
13. Svergun DI (1999) Restoring low resolution structure of biological macromolecules from solution scattering using simulated annealing. Biophys J 76:2879–2886.
14. Krissinel E, Henrick K (2007) Inference of macromolecular assemblies from crystalline state. J Mol Biol 372: 774–797.
15. Perugini MA, Griffin MD, Smith BJ, Webb LE, Davis AJ, Handman E, Gerrard JA (2005) Insight into the

self-association of key enzymes from pathogenic species. Eur Biophys J 34:469–476.
16. Pye VE, Tingey AP, Robson RL, Moody PC (2004) The structure and mechanism of serine acetyltransferase from *Escherichia coli*. J Biol Chem 279:40729–40736.
17. Svergun DI, Barberato C, Koch MHJ (1995) CRYSOL—a program to evaluate X-ray solution scattering of biological macromolecules from atomic coordinates. J Appl Cryst 28:768–773.
18. Svergun DI (1992) Determination of the regularization parameter in indirect-transform methods using perceptual criteria. J Appl Cryst 25:495–503.
19. Volkov VV, Svergun DI (2003) Uniqueness of ab-initio shape determination in small-angle scattering. J Appl Cryst 36:860–864.
20. Wriggers W, Chacon P (2001) Using Situs for the registration of protein structures with low-resolution bead models from X-ray solution scattering. J Appl Cryst 34: 773–776.